0090-9556/07/3508-1262–1268$20.00
DRUG METABOLISM AND DISPOSITION
Vol. 35, No. 8
14241/3228190
DMD 35:1262–1268, 2007
Printed in U.S.A.

Interaction of Positional Isomers of Quercetin Glucuronides with the Transporter ABCC2 (cMOAT, MRP2)

Gary Williamson, Isabelle Aeberli, Laurence Miguet, Ziding Zhang, M.-Belen Sanchez, Vanessa Crespy, Denis Barron, Paul Needs, Paul A. Kroon, H. Glavinas, Peter Krajcsi, and Martin Grigorov

Nestlé Research Center, Lausanne, Switzerland (G.W., I.A., L.M., Z.Z., M.B.S., V.C., D.B., M.G.); Institute of Food Research, Norwich, United Kingdom (P.N., P.A.K.); Solvo Biotechnology, Budapest, Hungary (H.G., P.K.); and Rational Drug Design Laboratories, Corporate Research Center, Budapest, Hungary (P.K.)

Received December 6, 2006; accepted May 2, 2007

ABSTRACT:

The exporter ABCC2 (cMOAT, MRP2) is a membrane-bound protein on the apical side of enterocytes and hepatic biliary vessels that transports leukotriene C_4, glutathione, some conjugated bile salts, drugs, xenobiotics, and phytonutrients. The latter class includes quercetin, a bioactive flavonoid found in foods such as onions, apples, tea, and wine. There is no available three-dimensional (3D) structure of ABCC2. We have predicted the 3D structure by in silico modeling, showing that 3-[[3-[2-(7-chloroquinolin-2-yl)vinyl]phenyl]-(2-dimethylcarbamoylethylsulfanyl)methylsulfanyl] propionic acid (MK571) binds most tightly to the putative binding site, and then tested the computational prediction experimentally by measuring interaction with all quercetin monoglucuronides occurring in vivo (quercetin substituted with glucuronic acid at the 3-, 3′-, 4′-, and 7-hydroxyl groups). The 4′-*O*-β-D-glucuronide is predicted in silico to interact most strongly and the 3-*O*-β-D-glucuronide most weakly, and this prediction is supported experimentally using binding and competition assays on ABCC2-overexpressing baculovirus-infected Sf9 cells. To test the transport in situ, we examined the effect of two ABCC2 inhibitors, MK571 and cyclosporin A, on the transport into the media of quercetin glucuronides produced intracellularly by Caco2 cells. The inhibitors reduced the amount of all quercetin glucuronides in the media. The results show that the molecular model of ABCC2 agrees well with experimentally determined ABCC2-ligand interactions and, importantly, that the interaction of ABCC2 with quercetin glucuronides is dependent on the position and nature of substitution.

ABCC2 (cMOAT, MRP2) is a member of the family of ATP binding cassette (ABC) transporters. Lack of ABCC2 expression in humans leads to the Dubin-Johnson syndrome, an autosomal dominant hereditary disease (König et al., 1999). This disease is manifested by chronic hyperbilirubinemia due to reduced biliary secretion of bilirubin conjugates (Payen et al., 2002). ABCC2 is a transmembrane protein that uses the energy of ATP hydrolysis to translocate its substrates across biological membranes and transports a wide variety of compounds, including various endobiotics and xenobiotics. Recent studies suggest that ABCC2 influences oral bioavailability (Dietrich et al., 2003), and its inhibition decreases the elimination of xenobiotics. It is structurally closely related to ABCC1 (MRP1) and the substrate selectivities of ABCC1 and ABCC2 overlap (Gerk and Vore, 2002) to a large extent.

The 1545-amino acid human ABCC2 contains two nucleotide-binding domains and up to 17 transmembrane helices distributed within three transmembrane domains (TMD), 1, 2, and 3. Classified in the same MRP family, human ABCC1 and human ABCC2 share 48% sequence identity as well as a similar membrane topology, implying structural and functional similarity. It has been shown that the amino-terminal TMD-1 of ABCC1 is not essential for substrate transport. Experimental efforts to characterize the substrate binding/transport have therefore been focused on transmembrane segments TM6 to TM17 of TMD-2 (TM6 to TM11) and TMD-3 (TM12 to TM17). To date, high-resolution 3D structures for ABCC1 and ABCC2 are still not available. The 3D structures for TMD-2 and -3 of ABCC1 have been obtained by homology modeling (Campbell et al., 2004). As revealed in the predicted 3D model, TMD-2 and -3 form a channel, which allows for the transportation of ABCC1 substrates. Together with biochemical studies, the 3D structural model for ABCC1 has provided further insight on the transport mechanisms (Campbell et al., 2004).

Quercetin is an anticarcinogenic flavonoid that affects phase II

Solvo Biotechnology has been supported by Grants FP6-2004-LIFESCI-HEALTH-5; Proposal No. 018961, FP6-2004-LIFESCIHEALTH-5; Proposal No. 518246, FP6, Network of Excellence (BioSim) 005137, and Hungarian Grants GVOP 3.1.1–2004-05-0506/3.0, GVOP 3.1.1–2004-05-0440/3.0, GVOP Munka–00034/2003, NKFP 1/A-041/04, RET, Debrecen, OTKA T 043141. P.N. and P.A.K. are supported by the Biotechnology and Biological Sciences Research Council, UK. G.W., I.A., L.M., Z.Z., M.B.S., V.C., D.B., and M.G. are, or were, employees of Nestlé SA, Switzerland.

Article, publication date, and citation information can be found at http://dmd.aspetjournals.org.

doi:10.1124/dmd.106.014241.

ABBREVIATIONS: ABC, ATP-binding cassette; MRP, multidrug resistance protein; TMD, transmembrane domain; TM, transmembrane; 3D, three-dimensional; MK571, 3-[[3-[2-(7-chloroquinolin-2-yl)vinyl]phenyl]-(2-dimethylcarbamoylethylsulfanyl)methylsulfanyl] propionic acid; HPLC, high-performance liquid chromatography; RMSD, root mean square deviation; UGT, UDP-glucuronosyl transferase.

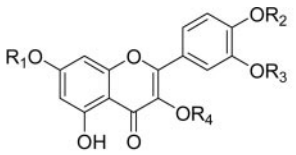

$R_1 = R_2 = R_3 = H$, R_4 = Gla: Quercetin 3-*O*-β-D-glucuronide
R_1 = Gla, $R_2 = R_3 = R_4 = H$: Quercetin 7-*O*-β-D-glucuronide
$R_1 = R_2 = R_4 = H$, R_3 = Gla: Quercetin 3'-*O*-β-D-glucuronide
$R_1 = R_3 = R_4 = H$, R_2 = Gla: Quercetin 4'-*O*-β-D-glucuronide

SCHEME 1. Gla, β-D-glucuronic acid.

enzyme-catalyzed detoxification, phosphorylation, and cell signaling (Uda et al., 1997; Nagasaka and Nakamura, 1998; Spencer et al., 2003). During metabolism, it is conjugated with glucuronide, methyl, and sulfate groups by the liver and small intestine (Gee et al., 2000; Day et al., 2001). Quercetin has five hydroxyl groups, and cellular glucuronidation of four of these (3-, 3′-, 4′-, and 7-positions) has been reported. A proportion of quercetin that is taken up by the enterocyte is effluxed back to the intestinal lumen in humans (Petri et al., 2003) and rats (Crespy et al., 1999). Glucuronide conjugation at the 3- and 7-positions reduces dramatically the inhibition of xanthine oxidase and lipoxygenase (Day et al., 2000), whereas glucuronide conjugation at the 3′- and 4′-positions reduces the ability to prolong the lag time of human low-density lipoprotein oxidation in vitro (Janisch et al., 2004). One of the factors limiting quercetin absorption could be the interaction of its glucuronides with pumps such as ABCC2, limiting the absorption by effluxing the conjugates back into the intestinal lumen or into the bile (Petri et al., 2003). MK571 has been used extensively as an inhibitor of ABCC2, e.g. (Pulaski et al., 1996), and cyclosporin is also an inhibitor (Wortelboer et al., 2003). We used a combination of quercetin conjugates and inhibitors to test interaction with ABCC2 and to assess the predictive power of an in silico generated 3D model of ABCC2.

Materials and Methods

Materials. Tamarixetin (4′-methylquercetin) and isorhamnetin (3′-methylquercetin) were purchased form Extrasynthese (Genay, France) (both >99% pure). The ABCC2 inhibitor MK571 and cyclosporin A were from Alexis Biochemicals (Lausan, Switzerland). Synthesis of conjugates enzymatically was as described previously (Morand et al., 1998; Day et al., 2000). Quercetin-7-*O*-β-D-glucuronide, quercetin-3-*O*-β-D-glucuronide, quercetin-3′-*O*-β-D-glucuronide, and quercetin-4′-*O*-β-D-glucuronide were chemically synthesized (Scheme 1) and characterized extensively as described previously (O'Leary et al., 2001; de Pascual-Teresa et al., 2004; Needs and Kroon, 2007).

HPLC. HPLC was performed using a Macherey-Nagel 100-5 C_{18} 250 mm × 3 mm column and a gradient of 15% acetonitrile + 0.5% H_3PO_4 + 84.5% water to 40% acetonitrile + 0.5% H_3PO_4 + 59.5% water over 15 min at 0.4 ml/min, with detection at 370 nm. Quercetin and conjugates were analyzed essentially as described previously (Day et al., 2001; Crespy et al., 2004).

Homology Modeling for TMD-2 and -3 in ABCC2. The fold identification for human ABCC2 (Swiss-Prot entry: Q92887) was performed via several fold recognition servers [FFAS (Jaroszewski et al., 1998), SAMT99 (Karplus et al., 1998), and Fugue (Shi et al., 2001)]. Although no structural templates for TMD-1 were identified, the structural templates for TMD-2 and -3 and two of the nucleotide-binding domains were confidently assigned. In our current investigation, we only focused on the structural modeling of TMD-2 and -3. All three of the fold recognition methods confidently assigned TMD-2 and TMD-3 to be structurally similar to the TMD in the lipid flippase MsbA (Chang, 2003) (a homolog of multidrug resistance ABC transporters, Protein Data Bank entry: 1pf4). The crystal structure of MsbA, solved at 3.8 Å resolution, consisted of a homodimer (chain A and B), where two of the TMDs were captured in a closed conformation. To build the 3D structures for TMD-2 and -3 of ABCC2, we took the TMD in chain A of 1pf4 as the template for TMD-2 and the TMD in chain B as the structural template for TMD-3. Because of the low sequence identity between ABCC2 (TMD-2 and -3) and 1pf4 (TMD), the alignments generated by the different fold recognition methods were quite different. As shown in Fig. 1, the alignments from fold recognition methods are much more similar than the ones obtained with ClustalW. Interestingly, the alignments from FFAS and SAMT99 were highly consistent, although the algorithms for constructing the alignments were different. Therefore, in the present study we used this consensual alignment for the homology modeling of TMD-2 and -3 of ABCC2. After a minor manual optimization of this alignment by an additional prediction of transmembrane helices, we built the 3D structure for TMD-2 and TMD-3 of ABCC2 by using WHAT IF software (Vriend, 1990). Furthermore, several small loops within the cavity formed by TMD-2 and -3 were built by using the Biopolymer module of the SYBYL modeling package (Tripos, St. Louis, MO). After refinement of the side chains, the addition of all hydrogen atoms, and energy minimization of the structure, the final 3D model of ABCC2 was generated (Fig. 2).

The validation of the ABCC2 model built by fold recognition methods consisted of evaluating whether it was able to recognize ABCC2 substrates and inhibitors. To reach this goal, a reference dataset of molecules consisting of 17 known ABCC1 and ABCC2 substrates and inhibitors was compiled (Table 1). This dataset was designed after careful inspection of the available literature using the SciFinder searching interface to the Chemical Abstracts Database. During the search no specific ABCC2 substrates and inhibitors were found. Most of them interacted with both ABCC1 and ABCC2 but at different effective concentrations.

Molecular Dataset with Quercetin Glucuronides. A second dataset, composed of quercetin-3-glucuronide, quercetin-3′-glucuronide, quercetin-4′-glucuronide, and quercetin-7-glucuronide, was built. Each molecule was manually designed and minimized with the SYBYL molecular modeling package using the Tripos force field to optimize these structures. As ABCC2 is a major canalicular organic anion transporter, the anionic form of the compounds was also investigated.

Virtual Screening of the Reference Data Base. We used two well known fixed protein-flexible ligand docking software packages, GOLD (Cambridge Crystallographic Data Centre, Cambridge, UK) and Glide (Schrödinger Inc., New York, NY) to perform molecular docking calculations on the ABCC2 model. First, a global docking calculation was carried out on the transporter with no a priori knowledge about the binding site location. This calculation was performed with the GOLD program as it permits the definition of a large binding site. In this step, the protein-binding site was defined as the whole transporter. For every molecule of the reference database, we used the software to generate one solution. Looking at the resulting conformations of the compounds, we focused on the known inhibitors. We identified the protein residues that make contact with the ABCC2 substrates and inhibitors. These residues form the potential binding site of the transporter: Lys^{329}, Met^{440}, Ser^{444}, Gln^{447}, Ile^{476}, Ile^{479}, Gln^{543}, Cys^{544}, Val^{546}, Phe^{550}, Thr^{553}, Val^{557}, Ser^{558}, Phe^{562}, Asn^{587}, Ile^{588}, Leu^{589}, Arg^{591}, Met^{595}, Met^{598}, Met^{599}, Trp^{1144}, Phe^{1149}, Trp^{1254}, Arg^{1257}, Met^{1258}, and Glu^{1260} (cf. Fig. 1). A second virtual screening calculation of the reference database was performed on the binding site defined above. The docking calculations were carried out with the GOLD and Glide docking software. For each, the same binding site was used, and 30 solutions were generated for each ligand. When considering the docking score of Glide (GlideScore) that estimates the binding affinity of the molecule to the protein, we have selected the first solution predicted for each ligand (Table 1). According to these results, the top-ranked molecules are ABCC2 inhibitors.

Interaction with ABCC2 in Vitro. Isolated membranes of ABCC2-expressing Sf9 insect cells were used to measure vanadate-sensitive ATPase activity during incubation with test compounds as described previously (Sarkadi et al., 1992; Bakos et al., 2000). The compounds were dissolved in 50% methanol as a 15 mM stock solution and tested between 13.7 and 300 μM. The maximum methanol concentration in the assay was 1%, and this had no effect on the assay. In activation studies, the capability of the compound to stimulate ATPase activity is determined, compared with the stimulatory effect of probenecid, a well known ATPase activator, as control. The maximal efficacy of the test compounds is expressed on a 0 to 100% scale, where 100% is defined as the activation observed in the presence of probenecid (1 mM). EC_{50} is defined as the concentration of the test compound needed to reach 50% of the maximal efficacy of the compound. In inhibition assays, the compounds

A

```
mrp2tmd2    KSGTKKDVPKSWLMKALFKTFYMVLLKSFLLKLVNDIFTFVSPQLLKLLISFASDRDTYL
TMH[a]      ----------------hhhhhhhhhhhhhhhhhhh-----------------------
samt99      .......WQTFKRLWTYIRLYKAGLVVSTIALVINAAADTYMISLLKPLLDEGF.GNAES
ffas        LHSDESNWQTFKRLWTYIRLYKAGLVVSTIALVINAAADTYMISLLKPLLDEGF.GNAES
fugue       .......WQTFKRLWTYIRLYKAGLVVSTIALVINAAADTYMISLLKPLLDEGFGNAESN
clustalw[b] .MSLHSDESNWQTFKRLWTYIRLYKAGLVVSTIALVINAAADTYMISLLKPLLDEGFGNA

mrp2tmd2    WIGYLCAILLFTAALIQSFCLQCYFQLCFKLGVKVRTAIMASVYKKALTLSNLARKEYTV
TMH         ---hhhhhhhhhhhhhhhhhh-------------------------------------
samt99      NFLRILPFMILGLMFVRGLSGFASSYCLSWVSGNVVMQMRRRLFNHFMHMPVRFFDQEST
ffas        NFLRILPFMILGLMFVRGLSGFASSYCLSWVSGNVVMQMRRRLFNHFMHMPVRFFDQEST
fugue       FLRIL.PFMILGLMFVRGLSGFASSYCLSWVSGNVVMQMRRRLFNHFMHMPVRFFDQEST
clustalw    ESNFLRILPFMILGLMFVRGLSGFASSYCLSWVSVVMQMRRRLFNHFMHMPVRFFDQEST

mrp2tmd2    GETVNLMSVDAQKLMDVTNFMHMLWSSVLQIVLSIFFLWRELGPSVLAGVGVMVLVIPIN
TMH         --------------------hhhhhhhhhhhhhhhhhhh----hhhhhhhhhhhhhhh
samt99      GGLLSRITYDSEQVAGATSRLVSIVREGASIIGLLTLMFWNSWQLSLVLIVVAPVVAFAI
ffas        GGLLSRITYDSEQVAGATSALVSIVREGASIIGLLTLMFWNSWQLSLVLIVVAPVVAFAI
fugue       GGLLSRITYDSEQVAGATSRALVSIVEGASIIGLLTLMFWNSWQLSLVLIVVAPVVAFAI
clustalw    GGLLSRITYDSEQVAGATSLVSIV REGASIIGLLTLMFWNSWQLSLVLIVVAPVVAFAI

mrp2tmd2    AILSTKSKTIQVKNMKNKDKRLKIMNEILSGIKILKYFAWEPSFRDQVQNLRKKELKNLL
TMH         hhhh----------------------------------------------------------
samt99      SFVSKRFRKISRNMQTAMGH.................................RQQTM
ffas        SFVSKRFRKISRNMQTAMGHVTSSAEQMLKGHKVVLSYGGQEVERKRFDKVSNSMRQQTM
fugue       SFVSKRFRKISRNMQTA.......MGHRQQTMKLVSAQSIADPVIQMIASLALFAVLFLA
clustal     SFVSKRFRKISRNMQTAMGHVTSSAEQMLKGHKVVLSYGGQEVERKRFDKVSNSMRQQTM

mrp2tmd2    AFSQLQCVVIFVFQLTPVLVSVVTFSVYVLVDSNNILDAQKAFTSITLFNILFRPLSMLP
TMH         -------hhhhhhhhhhhhhhhhhh----------------------hhhhhhhhhh
samt99      KLVSAQSIADPVIQMIASLALFAVLFLASVDSIRAELTPGTFTVVFSAMFGLMRPLKALT
ffas        KLVSAQSIADPVIQMIASLALFAVLFLASVDSIRAELTPGTFTVVFSAMFGLMRPLKALT
fugue       SVDSI.........................RAELTPGTFTVVFSAMFGLMRPLKALT
clustalw    KLVSAQSIADPVIQMIASLALFAVLFLASVDSIRAELTPGTFTVVFSAMFGLMRPLKALT

mrp2tmd2    MMISS
TMH         hhhhh
samt99      SVTSE
ffas        SVTSE
fugue       SVTSE
clustalw    SVTSE
```

B

```
mrp2tmd3    TGKVKFSIYLEYLQAIGLFSIFFIILAFVMNSVAFIGSNLWLSAWTSDSKIFNSTDYPAS
TMH         -------------hhhhhhhhhhhhhhhhhhh--------------------------
samt99      ........LWTYIRLYKA.GLVVSTIALVINAAADTYMISLLKPLLDEGFGNAESNF...
ffas        .....FKRLWTYIRLYKA.GLVVSTIALVINAAADTYMISLLKPLLDEGFGNAESN....
fugue       .....WQTFKRLWTYIRLYK..AGLVVSTIALVINAAADTYMISLLKPLLDEGFGNAESN
clusatlw    MSLHSDESNWQTFKRLWTYIRLYKAGLVVSTIALVINAAADTYMISLLKPLLDEGFGNAE

mrp2tmd3    QRDMRVGVYGALGLAQGIFVFIAHFWSAFGFVHASNILHKQLLNNILRAPMRFFDTTPTG
TMH         ---------------hhhhhhhhhhhhhhhhhhh-------------------------
samt99      .LRILPFMILGLMFVRGLSGFASSYCLSWVSGNVVMQMRRRLFNHFMHMPVRFFDQESTG
ffas        FLRILPFMILGLMFVRGLSGFASSYCLSWVSGNVVMQMRRRLFNHFMHMPVRFFDQESTG
clustalw    SNFLRILPFMILGFVRGLSGFASSYCLSWVSGNVVMQMRRRLFNHFMHMPVRFFDQESTG

mrp2tmd3    RIVNRFAGDISTVDDTLPQSLRSWITCFLGIISTLVMICMATPVFTIIVIPLGIIYVSVQ
TMH         --------------------hhhhhhhhhhhhhhhhhhh--hhhhhhhhhhhhhhhhhh
samt99      GLLSRITYDSEQVAGATSRALVSIVREGASIIGLLTLMFWNSWQLSLVLIVVAPVVAFAI
ffas        GLLSRITYDSEQVAGATSRALVSIVREGASIIGLLTLMFWNSWQLSLVLIVVAPVVAFAI
fugue       GLLSRITYDSEQVAGATSRALVSIVREGASIIGLLTLMFWNSWQLSLVLIVVAPVVAFAI
clustalw    GLLSRITYDSEQVAGATSRALVSIVREGASIIGLLTLMFWNSWQLSLVLIVVAPVVAFAI

mrp2tmd3    MFYVSTSRQLRRLDSVTRSPIYSHFSETVSGLPVIRAFEHQQRFLKHNEVRIDTNQKCVF
TMH         h---------------------------------------------------------
samt99      SFVSKRFRKISRNMQTAMGH.................................RQQTM
ffas        SFVSKRFRKISRNMQTAMGHVTSSAEQMLKGHKVVLSYGGQEVERKRFDKVSNSMRQQTM
fugue       SFVSKRFRKISRNMQTA.......MGHRQQTMKLVSAQSIADPVIQMIASL.........
clustalw    SFVSKRFRKISRNMQTAMGHVTSSAEQMLKGHKVVLSYGGQEVERKRFDKVSNSMRQQTM

mrp2tmd3    SWITSNRWLAIRLELVGNLTVFFSALMMVIYRDTLSGDTVGFVLSNALNITQTLNWLVRM
TMH         -------------hhhhhhhhhhhhhhhhhh---hhhhhhhhhhhhhhhhhh----
samt99      KLVSAQSIADPVIQMIASL.FVLFLASVDSIRAELTPGTFTVVFSAMFGLMRPLKAL...
ffas        KLVSAQSIADPVIQMIALFAVLFLASVDSIRAELTPGTFTVV.FSAMFGLMRPLKALTSV
fugue       ..................ALFAVLFLASVDSIRAELTPGTFTVVFSAMFGLMRPLKALTSV
clustalw    KLVSAQSIADPVIQMIASLALFAVLFLASVDRAELTPGTFTVVFSAMFGLMRPLKALTSV

mrp2tmd3    TSEIETNIVA
TMH         ----------
pdbblast    TSEFQRGMAA
samt99      ..........
ffas        TSEFQRGMAA
fugue       TSEFQRGMAA
clustalw    TSE.......
```

FIG. 1. Comparison of the sequence alignments based on different methods. a, the sequence alignment between TMD-2 and 1pf4 (Chain: A). b, the sequence alignment between TMD-3 and 1pf4 (Chain: B). [a]The prediction of transmembrane helices (TMHs) was taken from the annotation in the Swiss-Prot database. [b]For comparison, the alignment from classic sequence alignment method (i.e., ClustalW) was also displayed. mrp2tmd2 and mrp2tmd3 refer to the TMD-2 and -3 of MRP2, respectively. 1pf4 is the template lipid flippase protein, samt99, ffas, and fugue denote the sequence alignments obtained by different fold recognition algorithms. The residues in the proposed active site are in bold.

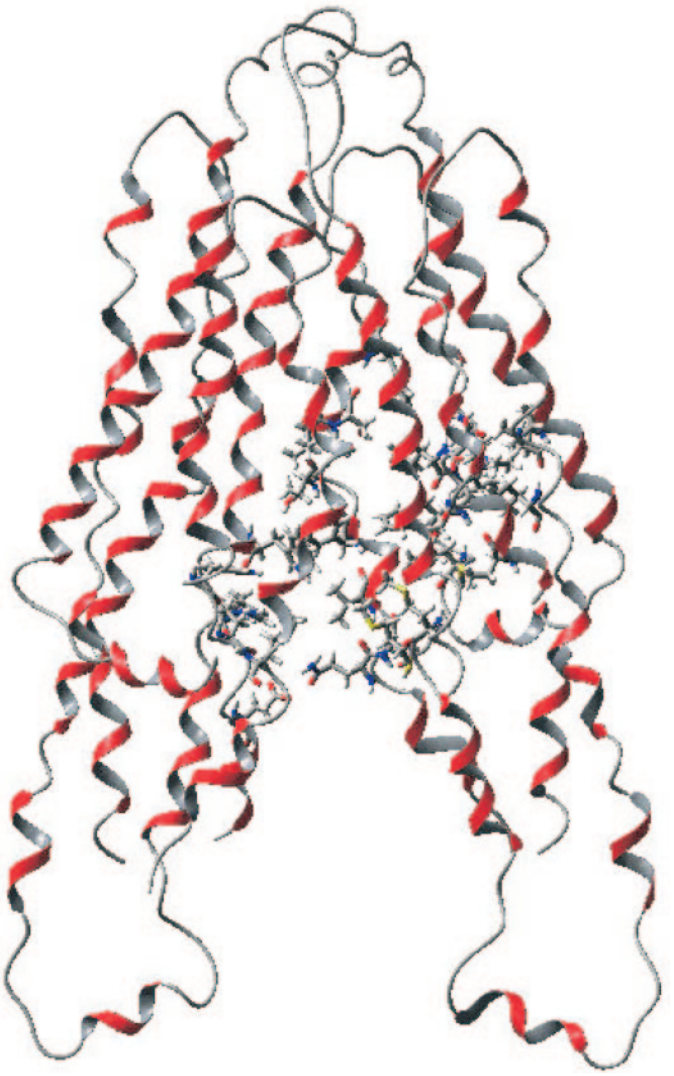

FIG. 2. Structure of the ABCC2 transporter generated in silico as described under *Materials and Methods*.

TABLE 1

Virtual screening results for the reference and the quercetin glucuronide datasets

Name	Anionic Form	Activity[a]	GlideScore[b]	RMSD[c]
MK571	Yes	Inhibitor	−11.11	1.73
Glibenclamide	No	Inhibitor	−8.93	1.86
SDZ-PSC 833	No	Inhibitor	−8.90	2.38
MK571	No	Inhibitor	−8.85	2.96
Verapamil	No	Inhibitor	−8.82	1.84
Quercetin-4′-*O*-β-D-glucuronide	Yes	Substrate	−8.6	1.75
Glycyrrhizin	No	Inhibitor	−8.59	2.10
Baicalin	No	Inhibitor	−8.59	2.19
Quercetin-7-*O*-β-D-glucuronide	Yes	Substrate	−8.52	1.37
Baicalin	Yes	Inhibitor	−8.41	1.03
Taxol (paclitaxel)	No	Inhibitor	−8.34	2.61
Quercetin-3′-*O*-β-D-glucuronide	Yes	Substrate	−8.28	1.59
Quercetin-3-*O*-β-D-glucuronide	Yes	Substrate	−7.66	1.34
Grepafloxacin	Yes	Substrate	−7.62	1.30
Ampicillin	No	Substrate	−7.39	2.51
Ampicillin	Yes	Substrate	−6.86	2.11
Quercetin	No	Substrate	−6.82	2.05
Grepafloxacin	No	Substrate	−6.74	2.19

[a] Activity toward ABCC2 according to the literature.
[b] Binding affinity, Glide energy units.
[c] RMSD between the energetically-preferred ("best") GOLD and Glide solution for each ligand.

TABLE 2

Interaction of quercetin glucuronides with ABCC2-overexpressed baculovirus-infected Sf9 cell membranes

	ATPase Activation[a]		ATPase Inhibition[a,b]	
	EC_{50}	Maximum Efficacy	EC_{50}	Maximum Efficacy
	μM	%	μM	%
Quercetin-7-*O*-β-D-glucuronide	61 ± 1.4	162.5 ± 53.0	55 ± 9.9	163 ± 89.1
Quercetin-3-*O*-β-D-glucuronide	100 ± 1.4	46.5 ± 6.4	95 ± 7.1	27 ± 9.9
Quercetin-3′-*O*-β-D-glucuronide	50 ± 22.6	85 ± 56.6		
Quercetin-4′-*O*-β-D-glucuronide	19 ± 1.4	48.5 ± 2.1	6 ± 1.4	72 ± 21.2

[a] Vanadate-sensitive ATPase activity in the absence of probenecid (basal activity) was 9.2 ± 2.3 nmol P_i/mg of protein/min. In the presence of 1 mM probenecid (activated ATPase) the vanadate-sensitive ATPase activity was 18.8 ± 2.0 nmol P_i/mg of protein/min.

[b] In inhibition experiments, the test compounds showed an ATPase activation that was additive with probenecid.

are tested for their ability to reduce the stimulatory effect of the control compounds on the respective ABC transporter. At least two independent experiments were carried out. EC_{50}, maximal efficacy, and S.D. were calculated.

Caco-2 Cell Culture. The cells were cultured in Dulbecco's modified Eagle's medium high glucose (4500 mg of glucose/l) with 20% fetal bovine serum, 100 U/ml penicillin-streptomycin, 1% nonessential amino acids, 1.25 μg/ml Fungizone and 50 μg/ml gentamicin in 10% CO_2 at 37°C. Cells were used at passages 29 to 35. Caco-2 cells were seeded into six-well plates at a density of 1×10^6 cells/well, the medium was changed every 2 days, and the experiments were carried out 20 d after cells reached confluence (Delie and Rubas, 1997). Quercetin was dissolved in dimethyl sulfoxide and added to the medium so that the final concentration of dimethyl sulfoxide added to the medium was 0.1%. On the day of the experiment, the cell culture medium was aspirated; the cells were washed with 2 ml of phosphate-buffered saline per well and then incubated with 2 ml of cell culture medium (without phenol red) with the addition of appropriate test compounds or dimethyl sulfoxide as a control. After incubation, the medium of each well was transferred into a 5-ml tube and immediately acidified with 20 μl of acetic acid (1 M), and aliquots of 50 μl were placed on dry ice to freeze and stored at −80°C. Samples were analyzed by HPLC as described above.

Results

The ABCC2 3D model was generated in silico as described above. We then performed an evaluation of its ability to recognize molecules that are known substrates of this transporter and that were included in our reference dataset. Because the binding mode of a ligand was initially unknown, a consensual approach was applied to predict the conformation of the molecules upon binding to the protein. For each ligand, the 30 conformations predicted by Glide were compared with the ones predicted by GOLD. A root mean square deviation (RMSD) value was calculated to compare the predicted solutions pair by pair. Generally, it is believed that two conformations with a RMSD value less than 2 Å are representative of the same binding mode. For every molecule, the solutions with the smallest RMSD values were retained. The results are presented in Table 1. Applying a cutoff of 2 Å for the RMSD, five molecules were selected. Four of the five turned out to be ABCC2 inhibitors, and the remaining one was an ABCC2 substrate. When ranking the molecules according to the GlideScore values, the best scoring solutions were found to be the ABCC2 inhibitors. This implies that the ABCC2 binding site residues make more favorable interactions with these molecules than with other ones from the reference dataset, such as the known ABCC2 substrates. In particular, the strongest ABCC2 inhibitor according to these docking studies was the anionic form of MK571. Some residues were identified to be in contact with all the inhibitors, such as Phe^{550}, Thr^{553}, Val^{557}, Asn^{587}, Ser^{558}, Trp^{1144}, and Phe^{1149}.

The inhibitors, baicalin and glycyrrhizin, contain one and two glucuronide moieties and form a hydrogen bond with the residues Arg^{1257} and Glu^{1260}. On the basis of the above validation of the ABCC2 transporter model, structure-based molecular docking experiments were performed to check the interaction with quercetin glucuronides. By using the same parameters applied in the validation step, the dataset containing the quercetin glucuronides (quercetin-3-*O*-β-D-glucuronide, quercetin-3′-*O*-β-D-glucuronide, quercetin-4′-*O*-β-D-glucuronide, and quercetin-7-*O*-β-D-glucuronide) was screened against the transporter model. Glide results are displayed in Table 1. According to their GlideScore values, it appears that they interact in a weaker way with the transporter than known ABCC2 inhibitors such as MK571.

We then tested the predictions from the in silico interactions in an in vitro assay. The ATPase assay monitors compound-induced activation of the transporter ATPase (Bakos et al., 2000). Good substrates activate the ATPase whereas inhibitors or slowly transported substrates can be detected by their inhibitory activity on the activated transporter. Therefore, the ATPase assay can be used to measure the interaction of ABCC2 with possible substrates or inhibitors (Table 2). Quercetin-7-*O*-β-D-glucuronide activated ABCC2 ATPase more efficiently than the positive control probenecid (162.5% versus 100%). This activation was *additive* with probenecid, because in the presence of this activator, maximal activity reached a plateau at around 250%. Quercetin-3-*O*-β-D-glucuronide was least effective in activating ABCC2, with an activity of 46.5% of the control and the EC_{50} at 100 μM. Coapplication with probenecid showed some cooperativity, but it was only significant at higher concentrations. There was some inhibition by quercetin-3-*O*-β-D-glucuronide below 30 μM and activation above that concentration. The activation was additive with probenecid. Quercetin-3′-*O*-β-D-glucuronide alone activated ABCC2 with a similar EC_{50}, but with activation only 50% of that of quercetin-7-*O*-β-D-glucuronide; on coapplication with probenecid, however, quercetin-3′-*O*-β-D-glucuronide showed no sign of any cooperativity or additivity in an inhibition-type experimental setup. Quercetin-4′-*O*-β-D-glucuronide elevated transporter-specific ATPase activity by 48.5% with a low EC_{50} value of 19 μM. However, the efficacy of the activation was less than the maximal activation seen with either quercetin-7-*O*-β-D-glucuronide or quercetin-3′-*O*-β-D-glucuronide because of the bimodal nature of the activation curve. Activation was additive with probenecid, because, in the presence of this bona fide activator, maximal activity peaked at 172% (Table 2).

A correlation between the experimental (EC_{50}) and in silico calculated (GlideScore) binding affinity values was calculated. The correlation was reasonably good given the limited number of substrates, with a correlation coefficient of 0.80, and implies that computational molecular docking methods might be used to estimate the binding energies of other molecules that interact with this protein.

To determine the effects of in situ location of the transporter on interactions, we measured the metabolism of quercetin. Quercetin enters cells probably by passive diffusion and is then conjugated in

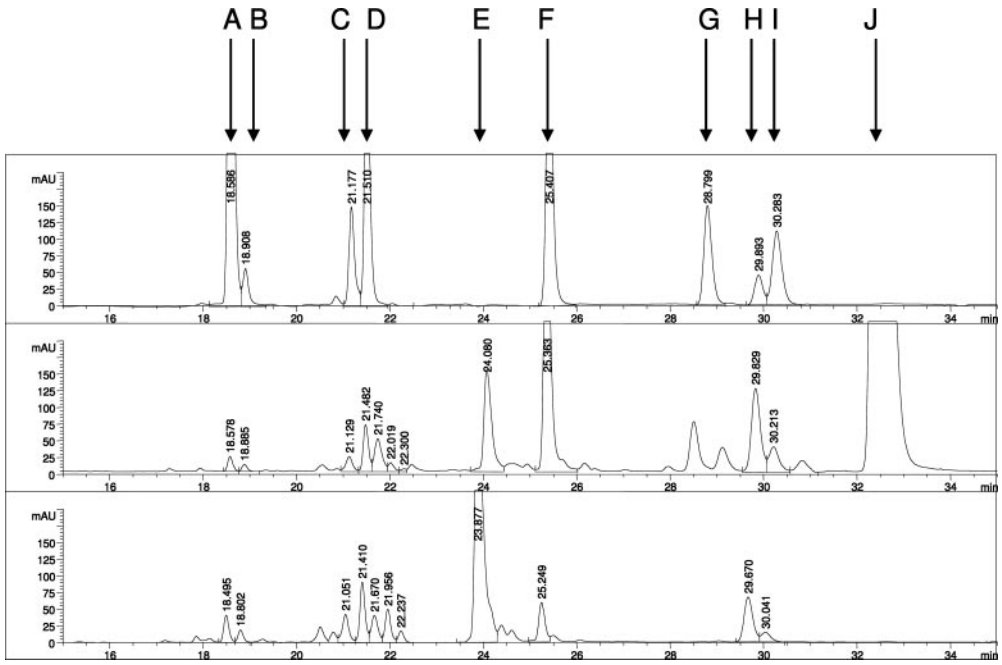

FIG. 3. HPLC chromatogram of quercetin metabolites. The top chromatogram shows the elution of a mixture of standards (A, B, C, D, F, G, H, and I). After incubation of quercetin with Caco-2 cells for 8 h, in the presence (middle chromatogram) and absence (lower chromatogram) of MK571, quercetin conjugates can be clearly seen. Peak E was identified as sulfate(s) because the peak disappeared after sulfatase treatment. Other peaks are indicated as follows: A, quercetin-3-*O*-*β*-D-glucuronide; B, quercetin-7-*O*-*β*-D-glucuronide; C, quercetin-4′-*O*-*β*-D-glucuronide; D, quercetin-3′-*O*-*β*-D-glucuronide; F, quercetin; G, apigenin (internal standard); H, 3′-methylquercetin; I, 4′-methylquercetin; J, MK571.

Caco-2 cells to form the methylated, glucuronidated, and/or sulfated conjugates. We propose that the glucuronides and possibly other conjugates are then effluxed by ABCC2 back into the medium. We tested the effect of the ABCC2 inhibitors, MK571 and cyclosporin A, on the efflux. In the presence of up to 0.5 mM MK571, there was no apparent toxicity because Caco2 cell viability was unaffected as measured using neutral red.

Figure 3 shows some example chromatograms of the cell culture medium after incubation with quercetin in the presence and absence of MK571. The latter appears as a large peak toward the end of the chromatogram. Using the information from the chromatograms, the rates of formation of conjugates were calculated (Fig. 4). Formation of quercetin 3- and 7-*O*-*β*-D-glucuronide and of 3′- and 4′-methylquercetin is not saturated because the amount produced doubles as the dose of quercetin was increased 2-fold. Quercetin 3′- and 4′-*O*-*β*-D-glucuronide conjugates are apparently saturated; i.e., the same amount of product is observed at both substrate concentrations (Fig. 4a). In the presence of the ABCC2 inhibitor, MK571, the profile of excreted metabolites is dramatically changed (Fig. 4b). In particular, quercetin-3-*O*-*β*-D-glucuronide and quercetin-7-*O*-*β*-D-glucuronide formations are abolished at both substrate concentrations and formations of quercetin-3′- and 4′-*O*-*β*-D-glucuronides are substantially decreased, demonstrating that MK571 blocks the transport of these compounds. In contrast, the formation or transport of 3′- and 4′-methylquercetin is unaffected or even increased in the presence of MK571 at the lower quercetin concentration. Quercetin sulfates were also products of Caco2 cell metabolism. The results represent one or more sulfates of unknown substitution position, but clearly these are important products of metabolism. The formation as measured by efflux into the cell culture medium is inhibited by MK571, which suggests that quercetin sulfate(s) is also a substrate for ABCC2. The results with cyclosporin A were qualitatively similar but less pronounced (results not shown).

Discussion

Several studies using a number of models have concluded that ABCC2 is an important efflux transporter for quercetin conjugates, and we have used these conjugates to understand the mechanism of ABCC2. Here, we have built the 3D structure of ABCC2 (mainly TMD-2 and -3) via homology modeling. After the building of a three-dimensional structure for the human ABCC2, the model was challenged by molecular docking experiments. On the basis of the above docking results, the ABCC2 model allowed discrimination of some ABCC2 inhibitors from some ABCC2 substrates. A virtual screening calculation using a large database of natural compounds could be envisaged to identify new ABCC2 inhibitors. There was a reasonable correlation between the experimental EC_{50} values for quercetin glucuronides and the GlideScore value that estimates the binding energy, obtained from the virtual screening experiments. Quercetin-3-*O*-*β*-D-glucuronide and quercetin-3′-*O*-*β*-D-glucuronide were predicted to have the weakest interaction by in silico modeling, and this prediction was supported experimentally by binding and competition assays on ABCC2-overexpressing baculovirus-infected Sf9 cells. Furthermore, in the intact Caco-2 cell metabolism experiment, MK571, an inhibitor of ABCC2, decreased the amount of all quercetin glucuronides effluxed into the cell culture medium. Any differences between results from the Caco-2 cells and the other methods are probably due to the complicating presence of other transporters and conjugating enzymes in the cells.

The ABCC2 transporter is expressed in Caco-2 cells (Gutmann et al., 1999) at physiological levels (Taipalensuu et al., 2001) and has been localized to the apical membrane of Caco-2 cells by immunofluorescence (Walgren et al., 2000). The presence of a glucuronide transporter is necessary for glucuronidation by UGT to be effective (Cummings et al., 2004). ABCC2 is also expressed in liver, kidney, enterocytes, placenta, and the blood-brain barrier, and its activity is inhibited by depletion of intracellular glutathione (Dietrich et al., 2003). ABCC2 interacts with a broad range of compounds, such as glucuronide conjugates of several molecules, including endogenous (leukotriene C_4, glutathione, and conjugated bile salts such as monoglucuronosyl and diglucuronosyl bilirubin) and exogenous (methotrexate, ochratoxin A, doxorubicin, cisplatin, and *S*-glutathionyl ethacrynic acid) compounds (Payen et al., 2002). ABCC2 is regulated by three distinct nuclear receptor signaling pathways (pregnane X receptor, farnesoid X-activated receptor, and constitutive androstane receptor) (Kast et al., 2002). Quercetin blocks As(III) up-regulation of ABCC2 mRNA in hepatocytes, possibly due to increased glutathione,

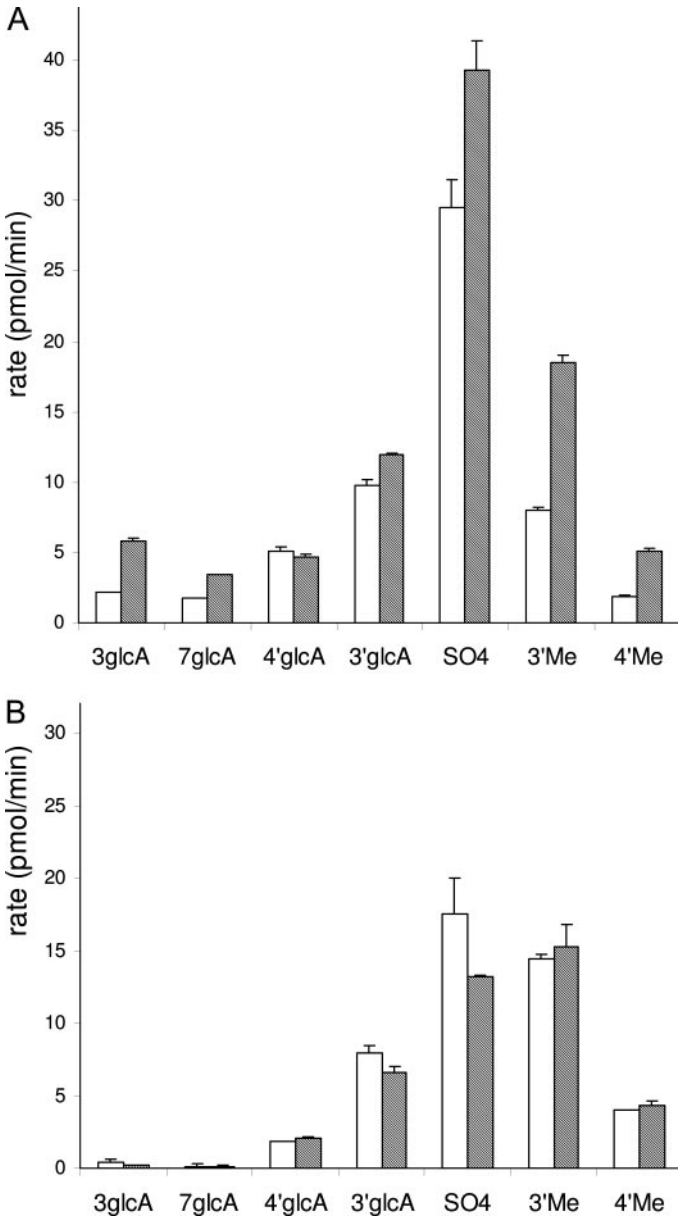

FIG. 4. Release of quercetin into Caco-2 cell culture medium in the (a) absence and (b) presence of MK571. The concentration of conjugate at 4 h was used to estimate a rate of the conjugation reaction. The initial quercetin concentration was 20 μM (open bars) or 40 μM (filled bars). The bar for sulfate is unassigned quercetin sulfate conjugates. The error bars indicate standard deviation ($n = 3$). 3glcA, quercetin-3-*O*-β-D-glucuronide; 7glcA, quercetin-7-*O*-β-D-glucuronide; 3′glcA, quercetin-3′-*O*-β-D-glucuronide; 4′glcA, quercetin-4′-*O*-β-D-glucuronide; SO4, mixed quercetin sulfates; 3′Me, 3′-methylquercetin; 4′Me, 4′-methylquercetin. At 4 h, the free quercetin concentrations in the medium were 2 and 9 μM after initial concentrations of 20 and 40 μM, respectively.

but not through effects on c-Jun NH_2-terminal kinase phosphorylation (Vernhet et al., 2001). Quercetin or *tert*-butyl hydroquinone coordinately induced UGT1A6 and ABCC2 in Caco-2 cells, whereas dioxin only induced UGT1A6, but not ABCC2 (Bock et al., 2000). Other polyphenols may interact with ABCC2; robinetin and myricetin effectively inhibited ABCC2, and the presence of a B-ring pyrogallol group was important for inhibition by the aglycone. Of importance, ABCC2 displayed a higher selectivity for flavonoid inhibition than ABCC1 (van Zanden et al., 2005). MK571 inhibited efflux of quercetin conjugates from HepG2 cells after treatment with quercetin-7-*O*-β-D-glucuronide and quercetin-3-*O*-β-D-glucuronide, although the quercetin-4′-*O*-β-D-glucuronide was not taken up into the cells (O'Leary et al., 2003). However, these experiments were very much dependent on the uptake of the conjugates by an organic anion transporter protein-like transporter. ABCC2 and ABCG2 (BCRP) are both involved in quercetin metabolism and disposition. ABCC2-deficient rats showed similar absorption of quercetin to the wild type, probably due to the compensating action of ABCG2 (Sesink et al., 2005).

It has been shown that ABCC2 has at least two binding sites. Positive cooperativity between substrates, as well as between substrates and nonsubstrates, is common (Bakos et al., 2000; Zelcer et al., 2003; Bodo et al., 2003), and MK571 potentiates the transport of estradiol-17β-glucuronide by ABCC2 (H. Glavinas, unpublished data). All of the quercetin conjugates activated the ABCC2 ATPase albeit with different potencies and efficacies. More interestingly, all but quercetin-3′-*O*-β-D-glucuronide showed an ATPase activation that seemed to be additive with probenecid-induced ABCC2 activation. An allosteric activation cannot therefore be completely ruled out. However, based on the correlation of the concentration dependence of ATPase activation and coactivation, allosteric activation is unlikely.

In summary, we have shown that an in silico generated structure of ABCC2 shows reasonable agreement with the experimentally determined binding of quercetin glucuronides. So far it has proven difficult to make reliable models for in silico prediction of ABCB1 (MDR1/Pgp)-substrate interactions. This work shows that transporters, possibly with stricter substrate specificities, such as ABCC2, are more amenable to model building.

References

Bakos E, Evers R, Sinko E, Varadi A, Borst P, and Sarkadi B (2000) Interactions of the human multidrug resistance proteins MRP1 and MRP2 with organic anions. *Mol Pharmacol* **57:**760–768.

Bock KW, Eckle T, Ouzzine M, and Fournel-Gigleux S (2000) Coordinate induction by antioxidants of UDP-glucuronosyltransferase UGT1A6 and the apical conjugate export pump MRP2 (multidrug resistance protein 2) in Caco-2 Cells. *Biochem Pharmacol* **59:**467–470.

Bodo A, Bakos E, Szeri F, Varadi A, and Sarkadi B (2003) Differential modulation of the human liver conjugate transporters MRP2 and MRP3 by bile acids and organic anions. *J Biol Chem* **278:**23529–23537.

Campbell JD, Koike K, Moreau C, Sansom MS, Deeley RG, and Cole SP (2004) Molecular modeling correctly predicts the functional importance of Phe^{594} in transmembrane helix 11 of the multidrug resistance protein, MRP1 (ABCC1). *J Biol Chem* **279:**463–468.

Chang G (2003) Structure of MsbA from *Vibrio cholera*: a multidrug resistance ABC transporter homolog in a closed conformation. *J Mol Biol* **330:**419–430.

Crespy V, Morand C, Manach C, Besson C, Demigne C, and Remesy C (1999) Part of quercetin absorbed in the small intestine is conjugated and further secreted in the intestinal lumen. *Am J Physiol* **40:**G120–G126.

Crespy V, Nancoz N, Oliveira M, Hau J, Courtet-Compondu MC, and Williamson G (2004) Glucuronidation of the green tea catechins, (−)-epigallocatechin-3-gallate and (−)-epicatechin-3-gallate, by rat hepatic and intestinal microsomes. *Free Radic Res* **38:**1025–1031.

Cummings J, Zelcer N, Allen JD, Yao D, Boyd G, Maliepaard M, Friedberg TH, Smyth JF, and Jodrell DI (2004) Glucuronidation as a mechanism of intrinsic drug resistance in colon cancer cells: contribution of drug transport proteins. *Biochem Pharmacol* **67:**31–39.

Day AJ, Bao Y, Morgan MRA, and Williamson G (2000) Conjugation position of quercetin glucuronides and effect on biological activity. *Free Radic Biol Med* **29:**1234–1243.

Day AJ, Mellon FA, Barron D, Sarrrazin G, Morgan MRA, and Williamson G (2001) Human metabolism of dietary flavonoids: identification of plasma metabolites of quercetin. *Free Radic Res* **212:**941–952.

Delie F and Rubas W (1997) A human colonic cell line sharing similarities with enterocytes as a model to examine oral absorption: advantages and limitations of the CaCo-2 model. *Crit Rev Ther Drug Carrier Syst* **14:**221–286.

de Pascual-Teresa S, Johnston KL, DuPont MS, O'Leary KA, Needs PW, Morgan LM, Clifford MN, Bao Y, Williamson G (2004) Quercetin metabolites downregulate cyclooxygenase-2 transcription in human lymphocytes ex vivo but not in vivo. *J Nutr* **134:**552–557.

Dietrich CG, Geier A, and Oude Elferink RP (2003) ABC of oral bioavailability: transporters as gatekeepers in the gut. *Gut* **52:**1788–1795.

Gee JM, DuPont MS, Day AJ, Plumb GW, Williamson G, and Johnson IT (2000) Intestinal transport of quercetin glycosides in rats involves both deglycosylation and interaction with the hexose transport pathway. *J Nutr* **130:**2765–2771.

Gerk PM and Vore M (2002) Regulation of expression of the multidrug resistance-associated protein 2 (MRP2) and its role in drug disposition. *J Pharmacol Exp Ther* **302:**407–415.

Gutmann H, Fricker G, Torok M, Michael S, Beglinger C, and Drewe J (1999) Evidence for different ABC-transporters in Caco-2 cells modulating drug uptake. *Pharmacol Res* **16:**402–407.

Janisch KM, Williamson G, Needs P, and Plumb GW (2004) Properties of quercetin conjugates: modulation of LDL oxidation and binding to human serum albumin. *Free Radic Res* **38:**877–884.

Jaroszewski L, Rychlewski L, Zhang B, and Godzik A (1998) Fold prediction by a hierarchy of sequence, threading, and modeling methods. *Protein Sci* **7:**1431–1440.
Karplus K, Barrett C, and Hughey R (1998) Hidden Markov models for detecting remote protein homologies. *Bioinformatics* **14:**846–856.
Kast HR, Goodwin B, Tarr PT, Jones SA, Anisfeld AM, Stoltz CM, Tontonoz P, Kliewer S, Willson TM, and Edwards PA (2002) Regulation of multidrug resistance-associated protein 2 (ABCC2) by the nuclear receptors pregnane X receptor, farnesoid X-activated receptor, and constitutive androstane receptor. *J Biol Chem* **277:**2908–2915.
König J, Nies AT, Cui YH, Leier I, and Keppler D (1999) Conjugate export pumps of the multidrug resistance protein (MRP) family: localization, substrate specificity, and MRP2-mediated drug resistance. *Biochim Biophys Acta* **1461:**377–394.
Morand C, Crespy V, Manach C, Besson C, Demigne C, and Remesy C (1998) Plasma metabolites of quercetin and their antioxidant properties. *Am J Physiol* **44:**R212–R219.
Nagasaka Y and Nakamura K (1998) Modulation of the heat-induced activation of mitogen-activated protein (MAP) kinase by quercetin. *Biochem Pharmacol* **56:**1151–1155.
Needs PW and Kroon PA (2007) Convenient synthesis of metabolically important quercetin glucuronides and sulfates. *Tetrahedron* **62:**6862–6868.
O'Leary KA, Day AJ, Needs PW, Mellon FA, O'Brien NM, and Williamson G (2003) Metabolism of quercetin-7- and quercetin-3-glucuronides by an *in vitro* hepatic model: the role of human β-glucuronidase, sulfotransferase, catechol-*O*-methyltransferase and multi-resistant protein 2 (MRP2) in flavonoid metabolism. *Biochem Pharmacol* **65:**479–491.
O'Leary KA, Day AJ, Needs PW, Sly WS, O'Brien NM, and Williamson G (2001) Flavonoid glucuronides are substrates for human liver β-glucuronidase. *FEBS Lett* **503:**103–106.
Payen L, Sparfel A, Courtois L, Vernhet A, Guillouzo A, and Fardel O (2002) The drug efflux pump MRP2: Regulation of expression in physiopathological situations and by endogenous and exogenous compounds. *Cell Biol Toxicol* **18:**221–233.
Petri N, Tannergren C, Holst B, Mellon FA, Bao Y, Plumb GW, Bacon J, O'Leary KA, Kroon PA, Knuson L, et al. (2003) Absorption/metabolism of sulforaphane and quercetin, and regulation of phase II enzymes, in human jejunum in vivo. *Drug Metab Dispos* **31:**805–813.
Pulaski L, Jedlitschky G, Leier I, Buchholz U, and Keppler D (1996) Identification of the multidrug-resistance protein (MRP) as the glutathione-S-conjugate export pump of erythrocytes. *Eur J Biochem* **241:**644–648.
Sarkadi B, Price EM, Boucher RC, Germann UA, and Scarborough GA (1992) Expression of the human multidrug resistance cDNA in insect cells generates a high activity drug-stimulated membrane ATPase. *J Biol Chem* **267:**4854–4858.
Sesink A, Arts I, de Boer V, Breedveld P, Schellens J, Hollman P, and Russel FG (2005) Breast cancer resistance protein (Bcrp1/Abcg2) limits net intestinal uptake of quercetin in rats by facilitating apical efflux of glucuronides. *Mol Pharmacol* **67:**1999–2006.
Shi J, Blundell TL, and Mizuguchi K (2001) FUGUE: sequence-structure homology recognition using environment-specific substitution tables and structure-dependent gap penalties. *J Mol Biol* **310:**243–257.
Spencer JPE, Rice-Evans C, and Williams RJ (2003) Modulation of pro-survival Akt/protein kinase B and ERK1/2 signaling cascades by quercetin and its in vivo metabolites underlie their action on neuronal viability. *J Biol Chem* **278:**34783–34793.
Taipalensuu J, Tornblom H, Lindberg G, Einarsson C, Sjoqvist F, Melhus H, Garberg P, Sjostrom B, Lundgren B, and Artursson P (2001) Correlation of gene expression of ten drug efflux proteins of the ATP-binding cassette transporter family in normal human jejunum and in human intestinal epithelial Caco-2 cell monolayers. *J Pharmacol Exp Ther* **299:**164–170.
Uda Y, Price KR, Williamson G, and Rhodes MJC (1997) Induction of the anticarcinogenic marker enzyme, quinone reductase, in murine hepatoma cells *in vitro* by flavonoids. *Cancer Lett* **120:**213–216.
van Zanden JJ, Wortelboer HM, Bijlsma S, Punt A, Usta M, Bladeren PJ, Rietjens IM, and Cnubber NH (2005) Quantitative structure activity relationship studies on the flavonoid mediated inhibition of multidrug resistance proteins 1 and 2. *Biochem Pharmacol* **69:**699–708.
Vernhet L, Seite MP, Allain N, Guillouzo A, and Fardel O (2001) Arsenic induces expression of the multidrug resistance-associated protein 2 (MRP2) gene in primary rat and human hepatocytes. *J Pharmacol Exp Ther* **298:**234–239.
Vriend G (1990) WHAT IF: a molecular modeling and drug design program. *J Mol Graph* **8:**52–56.
Walgren RA, Karnaky KJ Jr, Lindenmayer GE, and Walle T (2000) Efflux of dietary flavonoid quercetin 4′-β-glucoside across human intestinal Caco-2 cell monolayers by apical multidrug resistance-associated protein-2. *J Pharmacol Exp Ther* **294:**830–836.
Wortelboer HM, Usta M, van der Velde AE, Boersma MG, Spenkelink B, van Zanden JJ, Rietjens IM, van Bladeren PJ, and Cnubben NH (2003) Interplay between MRP inhibition and metabolism of MRP inhibitors: the case of curcumin. *Chem Res Toxicol* **16:**1642–1651.
Zelcer N, Reid G, Wielinga P, Kuil A, van der Heijden, I, Schuetz JD, and Borst P (2003) Steroid and bile acid conjugates are substrates of human multidrug-resistance protein (MRP) 4 (ATP-binding cassette C4). *Biochem J* **371:**361–367.

Address correspondence to: Dr. Gary Williamson, Nestlé Research Center, Vers Chez Les Blanc, 1000 Lausanne 26, Switzerland. E-mail: gary.williamson@rdls.nestle.com